Japanese Journal of Applied Physics

PROGRESS REVIEW

Orientation and size effects on phonon thermal conductivity in silicon/germanium multilayer structures

Japanese Journal of Applied Physics **62**, SD0804 (2023) **PROGRESS REVIEW**
https://doi.org/**10.35848/1347-4065/acad0c**

Orientation and size effects on phonon thermal conductivity in silicon/germanium multilayer structures

Alexander L. Khamets[1], Ivan I. Khaliava[1], Igor V. Safronov[2], Andrew B. Filonov[1], and Dmitri B. Migas[1,3*]

[1]*Belarusian State University of Informatics and Radioelectronics, 220089 Minsk, Belarus*
[2]*Belarusian State University, 220030 Minsk, Belarus*
[3]*National Research Nuclear University MEPhI (Moscow Engineering Physics Institute), Kashirskoe shosse 31, 115409 Moscow, Russia*

*E-mail: migas@bsuir.by

Received October 1, 2022; revised December 8, 2022; accepted December 19, 2022; published online January 18, 2023

We study the effect of morphology on the in- and cross-plane phonon thermal conductivity of the (001), (110), and (111) oriented Si/Ge multilayer films by means of non-equilibrium molecular dynamics at 300 K. The extended comparison of the estimated values for the multilayer films to one for the appropriate homogeneous Si and Ge films has been performed. The results revealed a significant advantage in reducing the thermal conductivity of the Si/Ge multilayer films compared to the referenced homogeneous Ge and Si films for the cross-plane transport regardless of the film orientation, and for the in-plane transport only for (001)/[$\bar{1}$10], (110)/[001] directions with an increase in the number of periods, which indicated the prospects of such layered structures.

1. Introduction

An increase in the thermoelectric figure of merit of Si or Si-based structures for use in thermoelectric devices is one of the actual trends in applied science during recent decades.[1)] An important advantage of using Si, and compounds with Si, lies in the well-established silicon technology, which allows for the formation of nanostructures in various forms, as well as the compatibility of Si and Ge with the standard integrated circuit manufacturing processes in comparison with traditional thermoelectric materials based on Te, Bi and Sb. The most important disadvantage of Si and Ge is their high thermal conductivity of ~140[2)] and ~55 W/(m·K)[3)] respectively, which makes it difficult to improve their thermoelectric efficiency.

To reduce such a high thermal conductivity, it is possible to use low-dimensional structures, such as thin films or nanowires,[4)] which allow for the scattering of a wide spectrum of phonons. Thus, in homogenous Si films significant decrease in the thermal conductivity (down to 10−20 W/(m·K)[5–7)]) can be achieved by reducing the film thickness to about 2−20 nm. Moreover, sizable anisotropy of the thermal conductivity in Si thin films was found in many studies highlighting specific crystallographic orientations associated with high or low values of thermal conductivity.[8–10)] Thus, the smallest thermal resistance in the in-plane direction of the film is found for the [110] direction of Si(110) films and the largest one—along the [111] direction of the Si(112) film.[8)] In Si nanomembranes, it was revealed that the highest in-plane thermal conductivity was achieved for the [100] direction of Si(011), but the difference between the values for the [100] and [011] directions was marginal (at 300 K), whereas the smallest value was detected along the [001] direction for Si(001).[9)] At the same time, the cross-plane thermal conductivity was the highest for the (111) oriented and the lowest for the (011) oriented structures, and values for the (001) oriented structures were quite comparable with the ones for the (011) oriented structures.[9)] It was noted that in (100), (110), (111) and (112) oriented thin Si films, a strong anisotropy of the in-plane thermal conductivity is typical of the (110) and (112) orientations (for [100], [110] and [110], [111] directions, respectively), while the lowest conductance is a characteristic of the (112)/[111] direction.[10)] Regarding homogenous Ge films, there are only a few papers[11,12)] reporting a significant anisotropy for the in- and cross-plane thermal conductivity depending on the film thickness[11)] and surface roughness.[12)] Recently, we have shown that for thin Ge films a trend similar to the one in thin Si films was observed, where the Ge (001) films in the [110] direction demonstrated the lowest values of thermal conductivity.[13)]

One of the promising nanostructures for thermoelectric applications could be a Si/Ge multilayer film (or a thin-film superlattice). In such structures, the internal interfaces are an additional factor of phonon scattering. A large number of papers were devoted to symmetric superlattices, in which the thermal conductivity was theoretically studied depending on the period.[14–21)] At the same time, as shown in many experimental papers[22–26)] the thermal conductivity could decrease even below 5 W/(m·K) in such (100) and (111) orientated structures. However, there are only a few papers devoted specifically to Si/Ge multilayer films with a small number of periods where the free surfaces are shown to act as an additional phonon scattering factor, and estimates only of the cross-plane thermal conductivity are reported.[27,28)] In our previous paper, the in-plane thermal conductivity in the (001), (110), and (111) orientated Si/Ge multilayer films along the [110] direction was considered.[13)] Thus, the effects of morphology (specific directions in differently oriented structures) on the phonon thermal conductivity in Si/Ge multilayer films still remain unclear, which is necessary for tuning the thermoelectric efficiency of devices based on them. The aim of this paper is to study systematically this issue for the cross- and in-plane phonon thermal conductivity in the (001), (110), and (111) orientated Si/Ge multilayer films compared to reference Ge and Si thin films of the equivalent thickness.

2. Simulation techniques

In this paper, we consider (001), (110), and (111) oriented Si/Ge multilayer films in the form of symmetric superlattices with sharp interfaces (excluding interdiffusion), as well as homogenous Si and Ge films of equivalent thickness. As a period we assumed the thickness of a Si/Ge bilayer. The

number of periods and the period itself are chosen as variable structural parameters. For the (001), (110), and (111) orientations, the p(2 × 1), p(1 × 1), and p(2 × 1) surface reconstructions were utilized, respectively, for both homogenous and layered films. The structures were prepared and visualized using the Jmol[29] and the OVITO[30] software.

All the structures were initially optimized by the molecular statics implemented in the LAMMPS software package.[31] The interatomic interaction for the Si–Ge system was described by using the Tersoff potential.[32] This potential predicts well the thermodynamic properties of Si and Ge bulks as well as Si–Ge solid solutions,[33] and it is widely used to simulate the thermal conductivity of Si/Ge films.[20,27,34,35] Three-dimensional periodic boundary conditions were used with a vacuum gap of ∼10 nm to simulate thin-film structure, and no gap was introduced to simulate bulk superlattices (infinite structures). The phonon component of thermal conductivity was simulated by non-equilibrium molecular dynamics also implemented in the LAMMPS software package.[31] The simulation was carried out in three stages. At the first stage, the structures were brought into thermodynamic equilibrium using at $T = 300$ K the isobaric-isothermal and canonical ensembles for 0.9 and 0.1 ns, respectively. In the second stage, a microcanonical ensemble was used to establish thermodynamic equilibrium for 2 ns. The Langevin thermostats were used to control the temperature in the layers, while the corresponding damping coefficients were introduced (for Ge atoms it is equal to 1, for Si atoms it is equal to 2.586 as the mass ratio), which affected the relaxation time during oscillations due to the difference in the masses of atoms. To introduce a temperature gradient in the structures we used two thermostats: a cold one ($T = 290$ K) and a hot one ($T = 310$ K) were placed at a distance of half of the size of the supercell in the direction of heat flow propagation for the in-plane thermal transport and at the ends of the structures for the cross-plane thermal transport. To stabilize the temperature, the number of atoms in both thermostats was kept the same (about 4800 atoms). In the third stage, the phonon thermal conductivity was evaluated, and the final value of the thermal conductivity was calculated after 2 ns of simulation, which was enough to assure our investigated structures were in a steady state. The calculation of the phonon thermal conductivity coefficient (κ_L) was determined from the Fourier law:

$$\kappa_L = -\frac{E}{2S_{sec} \cdot t \cdot (dT/dx)},$$

where E is the transferred thermal energy; 2 is the coefficient associated with the propagation of heat flow in two directions (only for the case of periodic boundary conditions); t is the simulation time; S_{sec} is the cross-sectional area; dT/dx is the temperature gradient.

When simulating the thermal conductivity in the direction of periodic boundary conditions, the supercell size was set to about 100 nm which is necessary to achieve a linear response mode between the inverse values of thermal conductivity and the supercell size.[13] The cross-sectional area for all the structures was chosen to be at least 60 nm.[2] Taking into account the phenomenon of thermal rectification, in our simulations of cross-plane thermal conductivity, the direction of the heat flow was set from Ge to Si in Si/Ge layered films due to lower thermal conductivity compared to the opposite direction.[27] Phonon band structures (dispersion curves) and group velocities are calculated using phonoLAMMPS[36] and Phonopy[37] softwares.

3. Results and discussion

Recently, in our previous paper[13] the in-plane thermal conductivity for some specific Si/Ge layered structures in comparison to Ge films was considered demonstrating its significant reduction in the [110] direction for the Si/Ge(100) multilayer films with the thickness over 13.6 nm. This effect occurred due to more intense phonon scattering with an increase in the number of interfaces compared to the Ge homogeneous film. Here we present the results of a more detailed and comprehensive analysis of the in- and cross-plane thermal conductivity of the Si/Ge layered structures. In particular, the following points are considered: the dependence of the conductivity for the (001), (110), and (111) oriented Si/Ge films in different directions on the period and the number of periods of the films; and the gain in the reduction of the conductivity for the layered structures as compared with the homogeneous films.

3.1. In-plane thermal conductivity of the Si/Ge layered structures

3.1.1. The thermal conductivity versus film thickness. Here the effects of surface orientations and specific directions on the in-plane thermal conductivity in Si/Ge layered structures are studied. In the first step, the (001), (110), and (111) oriented two-layer Si/Ge films of various thicknesses were considered, and the comparison with the appropriate Ge films was performed. We assumed here only layer-by-layer growth (the Frank-Van der Merwegrowth mode) of films, without considering island formation (due to the Stranski-Krastanov growth mode). In the case of the (001) orientation we consider only [110] direction, whereas for the (110) and (111) orientations the [001], [$\bar{1}$10] and [$\bar{1}$10], [$\bar{1}$12] directions are chosen, respectively (the inserts in Fig. 1). The results obtained demonstrate the orientation effect for the in-plane thermal transport in the considered layered structures. It is found that the lowest thermal conductivities are achieved in the cases of (001)/[$\bar{1}$10] and (110)/[001] directions (Fig. 1). With the decrease in the two-layer Si/Ge film thickness from 8 to 1–2 nm, a considerable decrease in the thermal conductivity is observed by a factor of 3 (from 15.7 to 5.11 W/(m·K)) or 2 (from 18.0 to 8.90 W/(m·K)) for the (001)/[$\bar{1}$10] and (110)/[001] directions, respectively, whereas only a slight decrease is found for the (110)/[$\bar{1}$10], (111)/[$\bar{1}$10], (111)/[$\bar{1}$12] directions (from 26.9 to 22.5, from 24.6 to 21.4, from 23.9 to 20.6 W/(m·K), respectively). When studying the in-plane thermal conductivity an interesting feature in the form of a crossover was found for the thicker two-layer Si/Ge films (not shown in Fig. 1). In particular, for the (110)/[001] direction, the thermal conductivity turned out to be 18.8 W/(m·K) at the film thickness of 15.7 nm, whereas for the (001)/[$\bar{1}$10] direction, the thermal conductivity was already equal to 18.9 W/(m·K) for the thinner film (13.3 nm). The reason for the crossover appearance in two-layer films can be the redistribution of contributions from phonon–interface and phonon–surface to phonon–phonon scattering with an increase in the thickness of the structures.

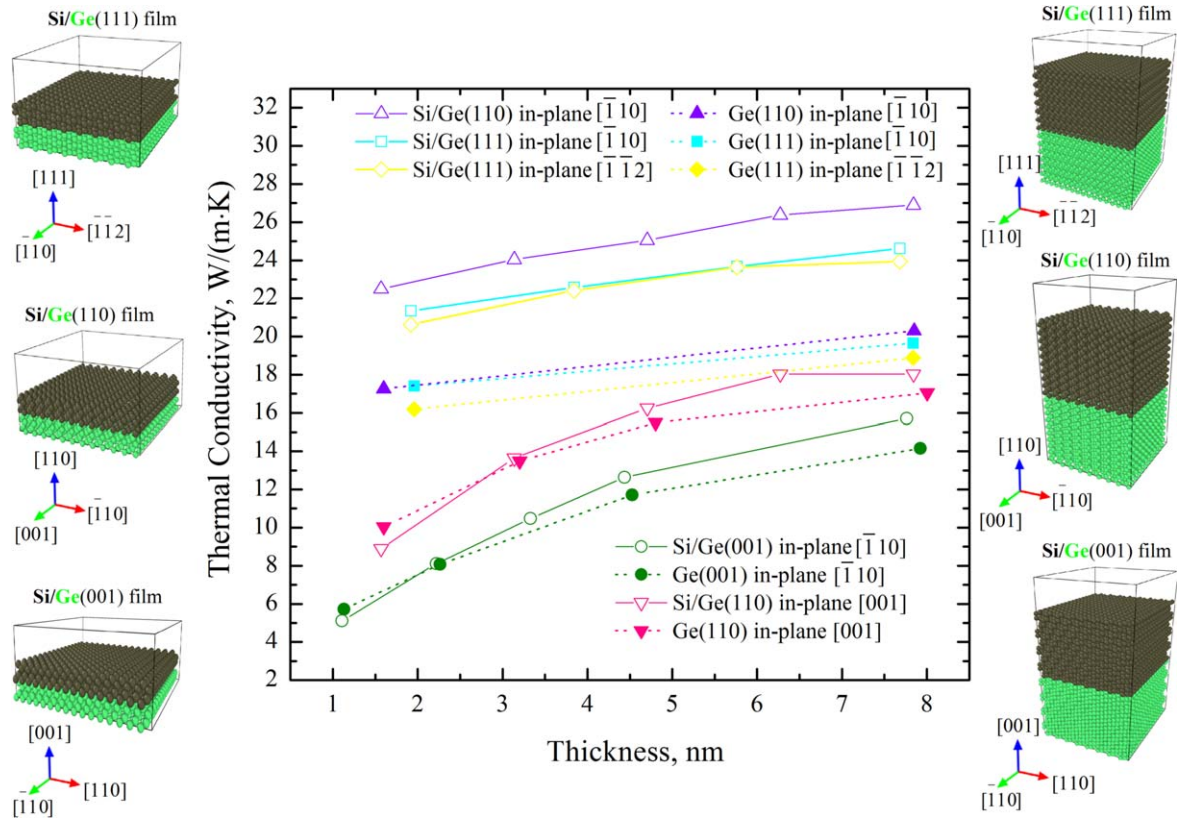

Fig. 1. (Color online) In-plane phonon thermal conductivity versus film thickness at 300 K for the two-layer Si/Ge films. The schematic structural models for the thinnest (the left column) and the thickest (the right column) films studied are also shown.

It is also revealed that in the two-layer Si/Ge films, the in-plane thermal conductivity is characterized by sizable anisotropy in the case of (110) orientated films contrary to the (111) case. Indeed, while the thermal conductivity differs by a factor of about 1.5–2.5 along the [$\bar{1}$10] and [001] directions for the (110) films, in the case of (111) films this difference is only a few percent (Fig. 1). The reason for that can be the different degree of anisotropy of the phonon group velocity, which depends on the shape of their isoenergetic surfaces, as shown for thin Si films.[10] Moreover, the obtained dependences can be explained by the difference in both the relaxation times of phonon–interface and phonon–surface scattering and the phonon group velocity for the films under consideration. Namely, due to the shape features of the phonon mode isoenergetic surfaces, inherent in cubic lattice structures (Si and Ge), the (110) surfaces have the lowest scattering capability contrary to (100) surfaces.[9] In addition, for ultrathin Si films the average phonon group velocities for the (001)/[$\bar{1}$10] and (110)/[001] directions are the lowest ones[10] in agreement with the cases considered here.

3.1.2. The thermal conductivity versus the number of periods. On the basis of data obtained from the (001)/[$\bar{1}$10] and (110)/[001] directions displaying the lowest in-plane thermal conductivity for the thinnest films (4 Si plus 4 Ge atomic monolayers), we further investigate the influence on the number of interfaces (or periods). Figure 2 shows the corresponding dependences of the thermal conductivity on the number of periods for Si/Ge multilayer films with a fixed period (8 atomic monolayers each) and the comparison with the appropriate Ge films. It is obvious that there is not only an orientation effect, but also a crossover of the dependences with an increase in the number of periods (Fig. 2). In the range from 1 to 4 periods, the thermal conductivity for the (001)/[$\bar{1}$10] direction is lower than for the (110)/[001] direction [5.11–11.6 W/(m·K) versus 8.90–12.4 W/(m·K)), whereas for n from 6 up to the bulk, the situation is vice versa (13.8–19.7 W/(m·K) versus 13.2–15.7 W/(m·K), respectively].

Even though one can expect that during the in-plane heat transfer layer-restricted phonons (propagate along the layers) contribute more to the thermal conductivity than extended phonons (propagate across the interfaces) do, there is an increase in the thermal conductivity with the number of periods due to the contribution of the extended phonons[18] (Fig. 2). This issue is also responsible for the appearance of the crossover in our multilayer Si/Ge films (Fig. 2) because of different saturation rates of the extended mode during thermal transport, depending on the phonon scattering for different directions. Note that previously, it was shown for thin Si films that the ballistic thermal conductance (diffusion processes were not taken into account) for the (110)/[100] direction was lower than the one for the (100)/[110] direction.[10]

In order to clarify the origin of the crossover, in Fig. 3 we present phonon band structures for multilayer Si/Ge films with the (001) and (110) orientations. It is obvious that for $n = 1$, the acoustic branch lies lower in frequency for the (001)/[$\bar{1}$10] direction than for the (110)/[001] one (indicated by rectangles in Fig. 3). This issue indicates the lower phonon group velocity in the former case and, as a consequence, the lower thermal conductivity. However, for the bulk Si/Ge superlattices, we observed the opposite

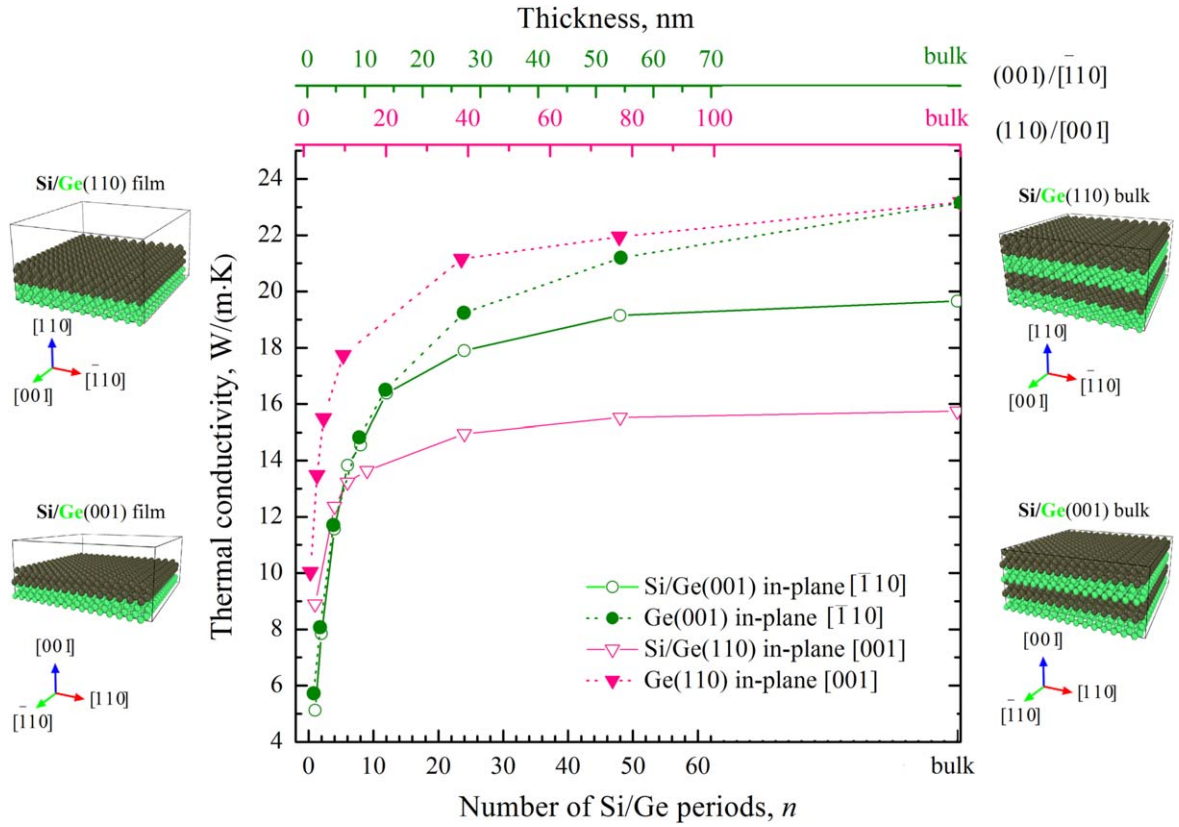

Fig. 2. (Color online) In-plane phonon thermal conductivity versus the number of periods at 300 K for multilayer Si/Ge films. The period is constant and equal to 1.1 and 1.6 nm for (001) and (110) orientated films, respectively. The schematic structural models of the films are also shown. Corresponding film thicknesses in nm are indicated on the upper axis.

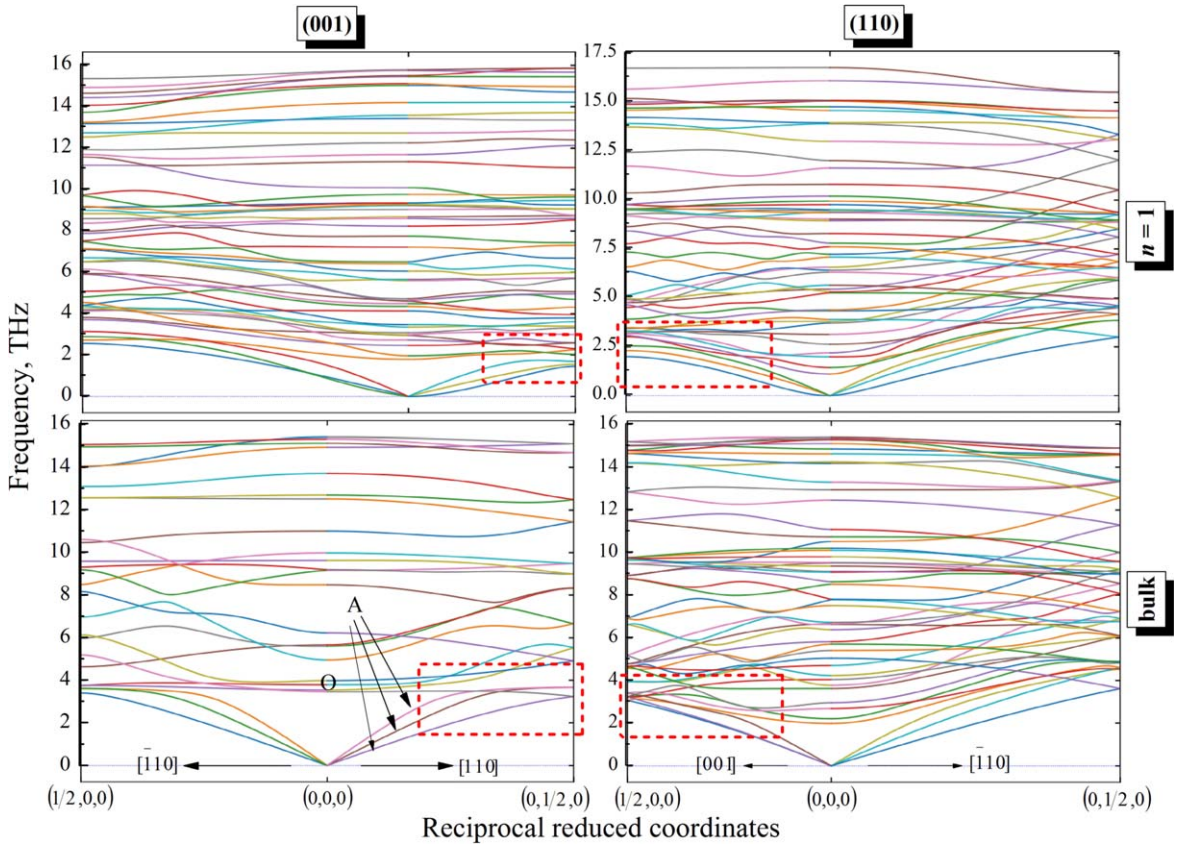

Fig. 3. (Color online) Phonon band structures for multilayer Si/Ge films with (001) and (110) orientations. Acoustic (A) and optical (O) branches are indicated.

situation (rectangles in Fig. 3) in addition to more strong optical–acoustic coupling[38,39] for the (110)/[001] direction and more effective phonon scattering.[38]

3.1.3. The gain in reducing the in-plane thermal conductivity: layered versus homogeneous films. And finally, the in-plane thermal conductivity of the Si/Ge layered films was compared with the corresponding homogenous Si and Ge films of equivalent thickness in the range of 1–8 nm. The results revealed that the two-layer Si/Ge films definitely had lower thermal conductivity (by 1.4–2.1 times) only compared to homogenous Si films for any direction (not shown in Fig. 1). However, the comparison to homogenous Ge films showed that the two-layer Si/Ge films had higher thermal conductivity by about 5–7 W/(m·K) for the (110)/[$\bar{1}$10] direction, by about 4–5 W/(m·K) for the (111)/[$\bar{1}$10], and (111)/[$\bar{1}\bar{1}$2] directions and up to about 1.5 W/(m·K) for the (001)/[$\bar{1}$10], and (110)/[001] directions (Fig. 1). But it is necessary to stress out that for the last two directions, there is a slight advantage (up to 0.6–1 W/(m·K)) in decreasing the thermal conductivity at small thicknesses (1–3 nm) for the two-layer Si/Ge films as compared to the appropriate Ge films (Fig. 1). Obviously, phonon–interface scattering in most cases does not compensate the contribution of the most heat-conducting Si layer during the in-plane thermal transport in the two-layer Si/Ge films. A comparison of the in-plane thermal conductivity of the Si/Ge multilayer films with small periods to one of the homogenous Ge films showed that as the number of periods was increased, the advantage in reducing the thermal conductivity was increased for the (001)/[$\bar{1}$10], (110)/[001] directions (Fig. 2). Such a difference in the in-plane thermal conductivity at $n = 48$ can reach 2.0 W/(m·K) for the (001)/[$\bar{1}$10] direction and 6.4 W/(m·K) for the (110)/[001] direction (Fig. 2). Eventually, it is clearly seen that the (110)/[001] direction displays the lowest values of the in-plane thermal conductivity at n more than 6 (Fig. 2).

3.2. Cross-plane thermal conductivity of the Si/Ge layered structures

In this section, the cross-plane thermal conductivity in (001), (110), and (111) oriented Si/Ge layered structures are studied. We start with two-layer films, which have almost equivalent thicknesses (by varying the number of monolayers in Si and Ge layers), to distinguish possible orientation effects. Despite the fact that the Si(100) surface has the highest phonon scattering capability,[9] a weak effect of the surface orientation on the cross-plane thermal transport in two-layer Si/Ge films, which is mainly determined by their thickness, has been established. As the thickness of these films decreases from 7.7 to 1.9 nm, the thermal conductivity decreases almost linearly by a factor of 3.5 [from 1.9 to 0.55 W/(m·K)] regardless of the crystallographic orientation. The latter means that the thermal transport is mainly ballistic when the mean free path of phonons is limited by the thickness of the layered film.[40] This has been previously reported both for homogenous Si films,[5,41] and for Si/Ge(001) multilayer films.[35] So, first of all, we consider the overall gain in the cross-plane thermal conductivity when using the Si/Ge layered structures as compared to homogeneous Si or Ge films. And then some other aspects, such as the influence of the period and the number of periods on the cross-plane thermal transport, are considered more in detail.

3.2.1. The gain in reducing the cross-plane thermal conductivity: layered versus homogeneous films. Taking into account that the main feature of cross-plane thermal transport is the reduction of phonon mean free path to the thickness of the film, it is important to elucidate a possible advantage of the considered layered films over homogenous Si and Ge films. First, we performed such a comparison for the two-layer films and the homogenous films with the equivalent thickness in the range of 1–8 nm for the (001), (110), and (111) orientated films. It has been found that the two-layer films have a clear advantage in suppressing cross-plane thermal conductivity not only compared to Si films, but also to Ge films over the entire thickness range (Fig. 4). This means that the phonon–interface scattering overcompensates the contribution of Si layers (having the highest thermal conductivity as compared to Ge layers) to the overall thermal conductivity. Note that this effect increases with increasing the film thickness. For example, the thermal conductivity of the two-layer Si/Ge(001) films is lower than the one for the Ge(001) film by a factor of 2 (for the Si film by 2.8) for the film thicknesses of 1.1 nm, and by a factor of 2.5 (for the Si film by 3.9) for the film thickness of 6.5 nm [Fig. 4(a)]. While homogenous Si(001) and Ge(001) films no longer meet the so-called criterion of the amorphous limit in the thermal conductivity [about 1 W/(m·K)[42]) at the film thicknesses of about 1–2 nm, for the two-layer Si/Ge(001) films this range expands up to about 5 nm [Fig. 4(a)], which makes it possible to tune the thermoelectric properties, avoiding the influence of quantum confinement effects on electronic properties. It is necessary to notice, that similar trends were observed for the (110) and (111) oriented films as well [Figs. 4(b) and 4(c)].

In order to trace the effect of the interface number (number of periods), the comparison of the cross-plane thermal conductivity for the two-layer and multilayer Si/Ge films with equivalent thickness was performed. In Figs. 4(a)–4(c) it is clearly seen that the difference in the thermal conductivity for the two- and multilayer Si/Ge films was increased when increasing the period number due to the enhancement of phonon–interface scattering. For example [Fig. 4(a)], at $n = 6$, this difference is as high as 0.41 W/(m·K) (which is about 24% of the conductivity value). It is also found that for the Si/Ge multilayer films, the thermal conductivity can be further reduced by choosing the material of the terminating surfaces (especially for the structures with n larger than 6) [Fig. 4]. The results show that in the case of Si-terminated surfaces [Si/Ge/…/Si structures, Fig. 4(a)], with an increase in the number of periods from 6 to 48, it is possible to reduce the thermal conductivity of ordinary Si/Ge(001) multilayer films by 0.76 W/(m·K) (which is about 13% of the conductivity value). Despite the fact that the Si layer is more "thermally conductive," the multilayer films with Ge-terminated surfaces (Ge/Si/…/Ge structures) have a higher thermal conductivity compared to Si/Ge/…/Si structures [Fig. 4(a)]. Moreover, the difference in thermal conductivity also increases with the number of periods for these structures. The latter effect is due to the fact that ballistic thermal transport prevails in the Ge/Si/Ge structures, while diffusion thermal transport prevails in the Si/Ge/Si structures, which affects the thermal resistance of interfaces.[35,43] Similar trends concerning an additional decrease in thermal conductivity (up

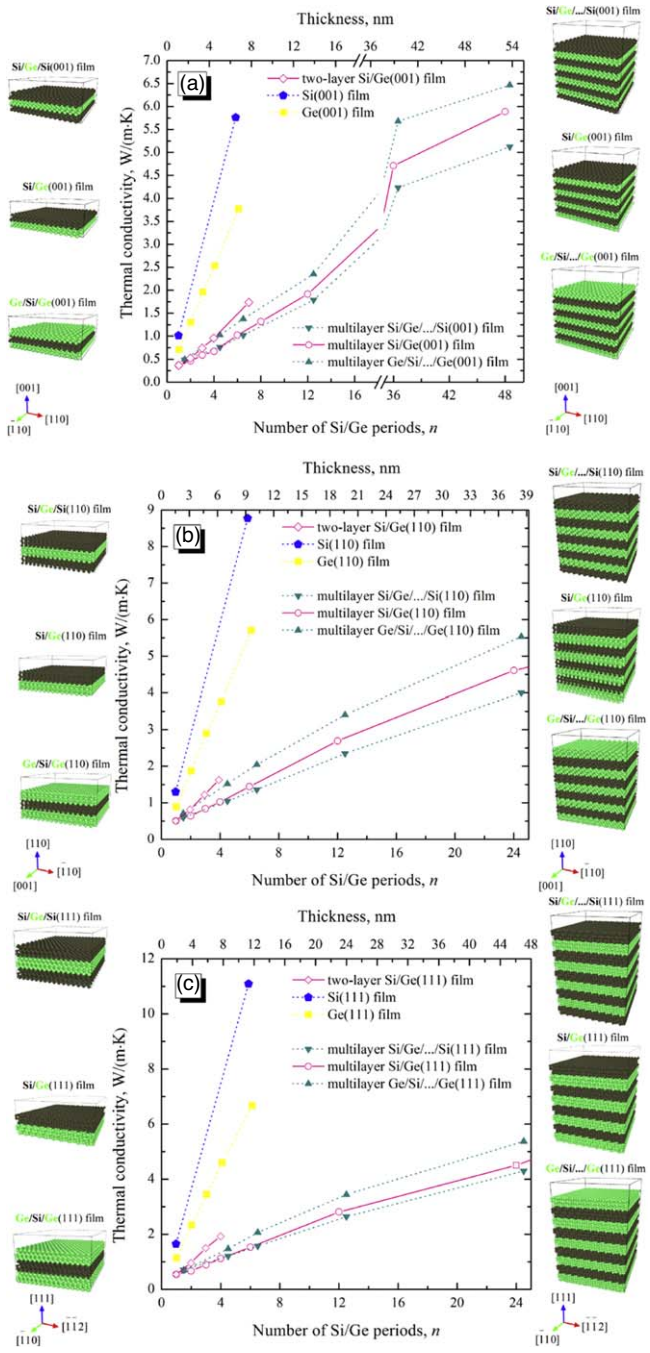

Fig. 4. (Color online) Cross-plane phonon thermal conductivity versus the number of periods or film thickness at 300 K and the schematic structure models of the films: (a) in the [001] direction; (b) in the [110] direction; (c) in the [110] direction. Corresponding film thicknesses in nm are indicated on the upper axis.

to about 5%–15% of the conductivity value) with an increase in the period number in Si/Ge multilayer films due to Si-terminated surfaces are also typical of the (110) and (111) orientations [Figs. 4(b) and 4(c)].

3.2.2. The thermal conductivity versus the number of periods. The surface orientation effect is also traced for Si/Ge multilayer films with a fixed period, i.e. 8 monolayers for (001), (110), and 12 monolayers for (111) orientated films, respectively, which are characterized by a large number of interfaces (Fig. 5). It is found that in multilayer films the surface orientation effect on the cross-plane thermal conductivity increases with the number of periods due to more intense phonon–interface scattering (Fig. 5). Increasing thermal conductivity in the cases, where the effective phonon mean free path is limited by the size of multilayer structure, is due to the existence of phonons capable of propagating ballistically within the structure, and the deviation from the linear dependence occurs because of the presence of phonons propagating diffusionally.[28,44,45] Thus, as the number of periods decreases from the bulk to 1, the cross-plane thermal conductivity decreases by more than an order of magnitude: from 6.36 to 0.363 W/(m·K), from 6.67 to 0.504 W/(m·K), and from 5.44 to 0.546 W/(m·K) for (001), (110) and (111) orientated films, respectively. The presence of a crossover is also revealed (Fig. 5): in the range from 1 to ∼40 periods, the (001) orientation possesses the lowest thermal conductivity, and with a further increase in the number of periods, the (111) orientation shows the lowest thermal conductivity. It can be explained by the presence of the (001) surface effectively scattering phonons and by the saturation in the thermal conductivity for the (111) orientated films with the increasing number of periods since the phonon scattering at the interfaces intensifies (Fig. 5). Here, we note that in the case of the cross-plane thermal transport, the increase in the thermal conductivity of multilayer films with a number of periods is due to an increase in the effective phonon mean free path which gradual approaches to its saturation.[28,44]

Based on the concept of the layer-restricted and extended modes of thermal transport in layered films,[18] it can be assumed that the reason for the appearance of the crossover is the difference in the saturation rates of the extended mode, depending on the effective mean free path of phonons, for various directions. With the cross-plane heat transfer, extended phonons provide the main contribution to the thermal conductivity compared to the layer-restricted ones.[18] In this case, the influence of both the group velocity and the relaxation time of phonons on the cross-plane thermal conductivity is strong due to the coincidence of the phonon propagation direction with the scattering direction. Note that the periodicity of the structure plays an important role in this issue.

3.2.3. The thermal conductivity versus period for the bulk Si/Ge superlattices. The significant effect of the period on the cross-plane thermal conductivity for the (001), (110), and (111) oriented Si/Ge superlattices without surfaces is shown in Fig. 6. First of all, there is a decrease in the thermal conductivity with a decrease in the period due to an increase in the phonon–interface scattering rate (density of interfaces increases),[14–16,20,28,44,46] followed by an increase in the thermal conductivity, which is associated with the phonon coherence effect[14–16,19,46–51] indicating the presence of a minimum in thermal conductivity values (Fig. 6). The appearance of so-called coherent phonons is caused by interference (the wave nature) of the incident and reflected phonons due to the increasing role of their mirror scattering from interfaces when the specific value of the period is reached. The physical reason for the appearance of the thermal conductivity minimum is interpreted as the largest achievable decrease in the phonon group velocity due to the dispersion curve flattening attributed to Brillouin-zone folding.[46–48] Regarding the relaxation time of phonon–surface/interface scattering, (110) and (100) surfaces/interfaces have the lowest and largest scattering capability,

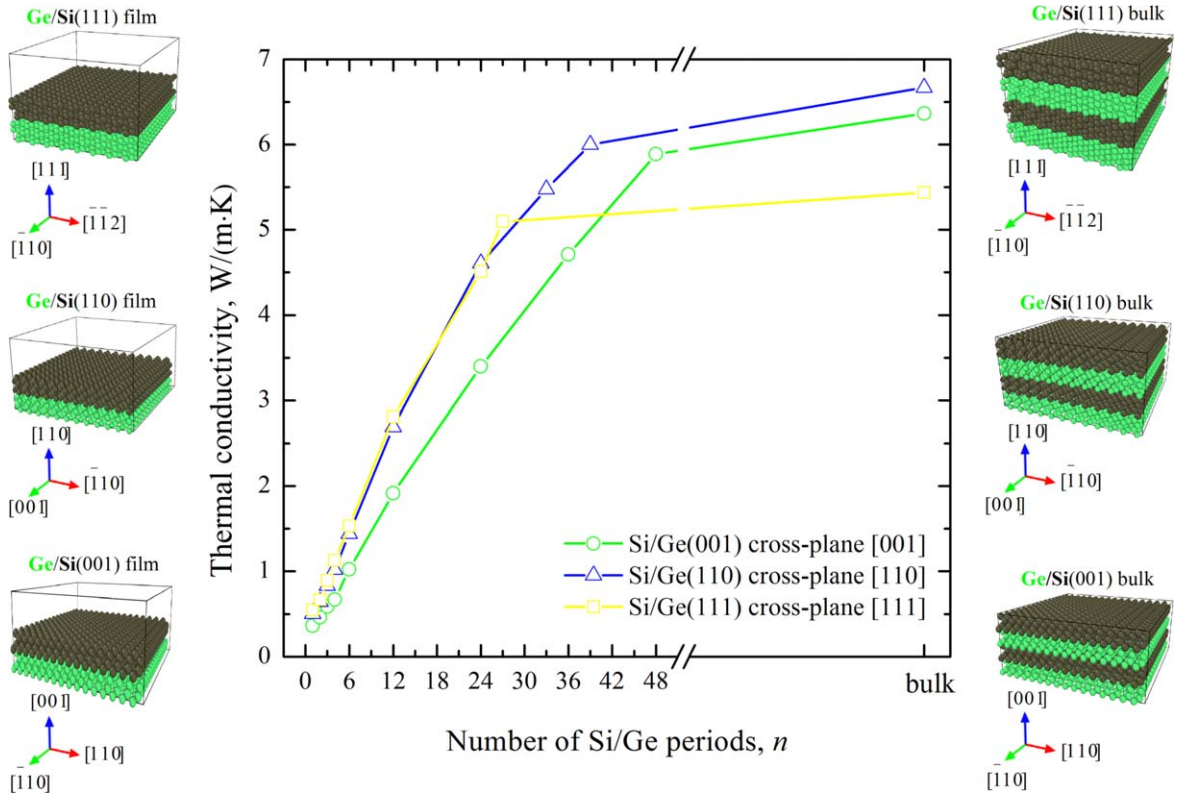

Fig. 5. (Color online) Cross-plane phonon thermal conductivity versus the number of periods at 300 K for multilayer Si/Ge films. The period is constant and equal to 1.1, 1.6 nm for (001), (110) orientated films (8 monolayers), and 1.9 nm for (111) orientated films (12 monolayers).

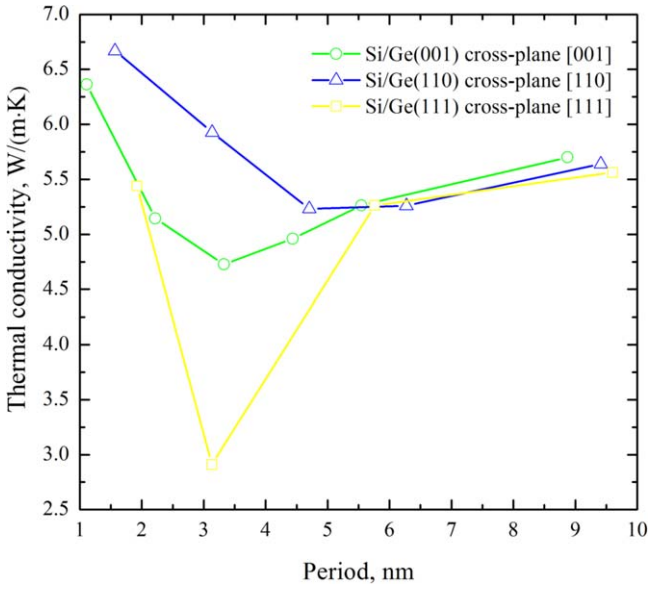

Fig. 6. (Color online) Cross-plane phonon thermal conductivity versus period at 300 K for the Si/Ge bulk superlattices.

respectively.[9] Thus, for bulk superlattices, both the surface orientation and the period play an essential role. To prove this statement in Fig. 7 we show the dependence of cross-plane group velocities on the phonon frequency for bulk Si/Ge superlattices. Even though the [001] direction is characterized by higher group velocities with respect to the [110] direction (the left column in Fig. 7), the TA-phonons are effectively scattered on (001) interfaces, whereas scattering of LA-phonons[17] is typical of the [111] direction for the (111) interfaces that explains maximal and minimal cross-plane thermal conductivity for the bulk Si/Ge(110) and Si/Ge (111) superlattices, respectively. By increasing the period (the right column in Fig. 7) the corresponding curves shift towards lower frequencies indicating a further decrease in thermal conductivity except for the case of the bulk Si/Ge (111) superlattice where almost all branches disappear (only the TA one is left) that clarifies the abrupt decrease in the cross-plane thermal conductivity (Fig. 6). We emphasize that the dependences of Fig. 6 predict the thermal conductivity trends of Si/Ge multilayer films with a large number of periods (from several dozens of periods to the bulk, Fig. 5).

Because the Si/Ge layered structures fabricated experimentally are bulk-like superlattices due to their large thickness (from several hundreds of nm to a few microns), a direct comparison of the calculated values with the experimental ones is not straightforward in the range of a small number of periods, at which low thermal conductivity is achieved. Nevertheless, a satisfactory agreement can be traced between our results and experimental values for the cross-plane thermal conductivity of Si/Ge bulk superlattices with (001)[22–24] and (111)[25] orientations. Moreover, our estimated values of the cross-plane thermal conductivity are close to the data obtained for Si/Ge(001) multilayer films by non-equilibrium molecular dynamics[27] as well as to the other results[14–16,19–21] for bulk superlattices.

3.2.4. The thermal conductivity versus period and number of periods. Taking into account the data obtained for bulk superlattices, it is interesting to consider the influence of both the period and the number of periods in the Si/Ge multilayer films with the (001) orientation as an example. The results are presented in Fig. 8 indicating the transition of the thermal transport from incoherent to coherent with the increase in the number of periods in Si/Ge multilayer

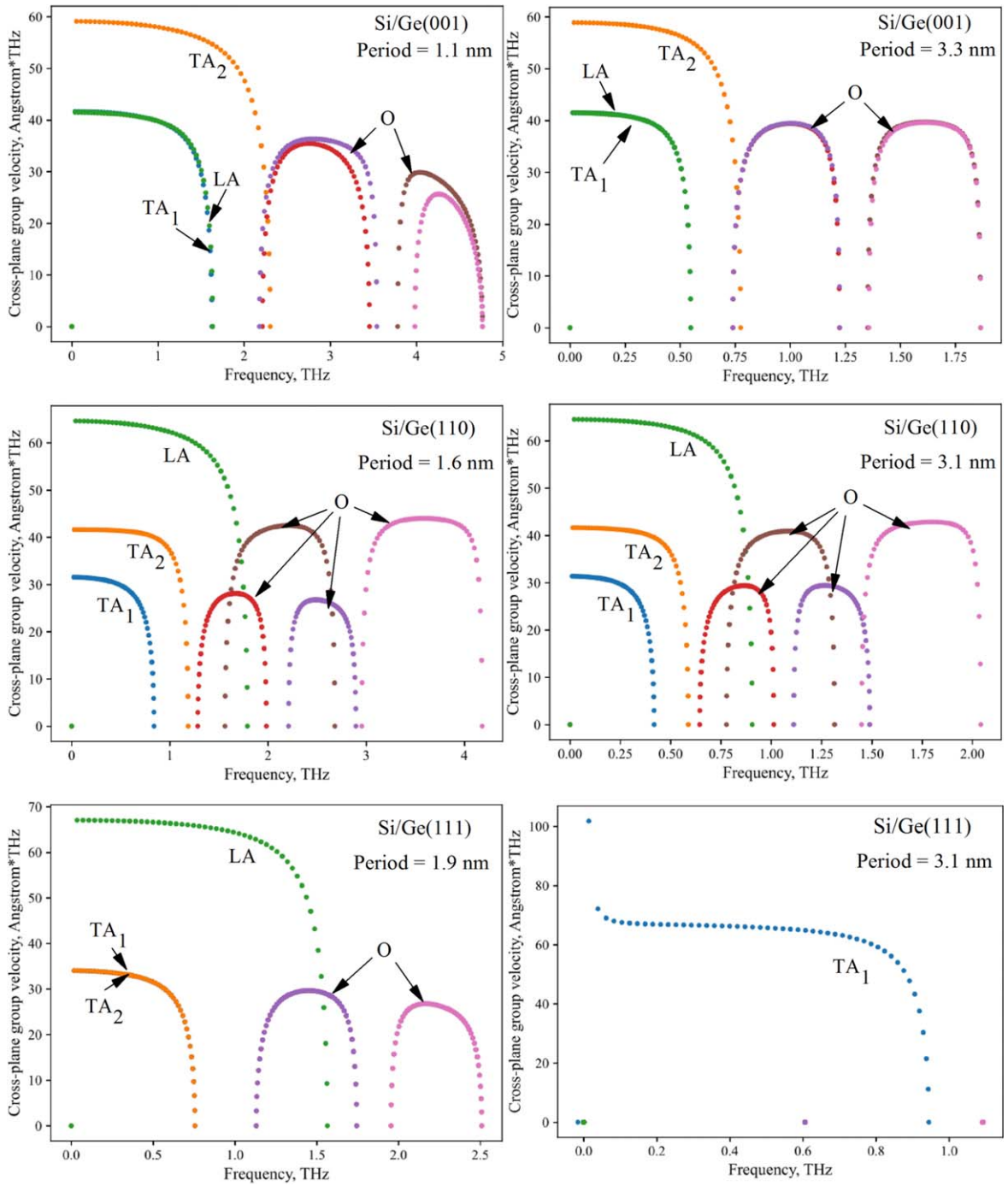

Fig. 7. (Color online) Frequency dependences of cross-plane group velocities for the first 7 branches for bulk Si/Ge superlattices at the smallest and almost equivalent periods.

films and having various periods. According to the original works,[48,49,51] in superlattices the transition of cross-plane thermal transport from coherent to incoherent is characterized by the presence of a minimum in the dependence of the thermal conductivity with respect to the period (as in Fig. 8). Here we emphasize that this effect significantly depends on the number of periods in a multilayer film, taking into account the wave nature of the interference of phonons.[46,48–50] Figure 8(a) shows the crossover of dependencies with periods of 8, 16 and 24 monolayers (solid lines with empty symbols), which is not observed with a further increase in the period (dashed lines with filled symbols). With an increase in the number of periods in Si/Ge multilayer films, phonon transport is partly ballistic, partly diffusive. Upon reaching a certain number of periods ($n \sim 22$, ~ 34) in structures with a specific period at which the phonon–interface scattering rate is higher, phonons begin to interfere when passing through the interfaces. We observe this at the crossover points of the dependencies, where the color of the solid lines changes from blue to green or yellow [Fig. 8(a)]. In addition, Fig. 8(b) shows how the dependences of the conductivity with respect to the period in the Si/Ge(001) multilayer films are qualitatively transformed as the number of periods (and total size) increases. A characteristic minimum does not appear in the dependences immediately, since it starts manifesting at $n > 22$, where color identification tells which section is dominated by incoherent (blue) or coherent (green) thermal transport [Fig. 8(b)]. At $n = 12$, the

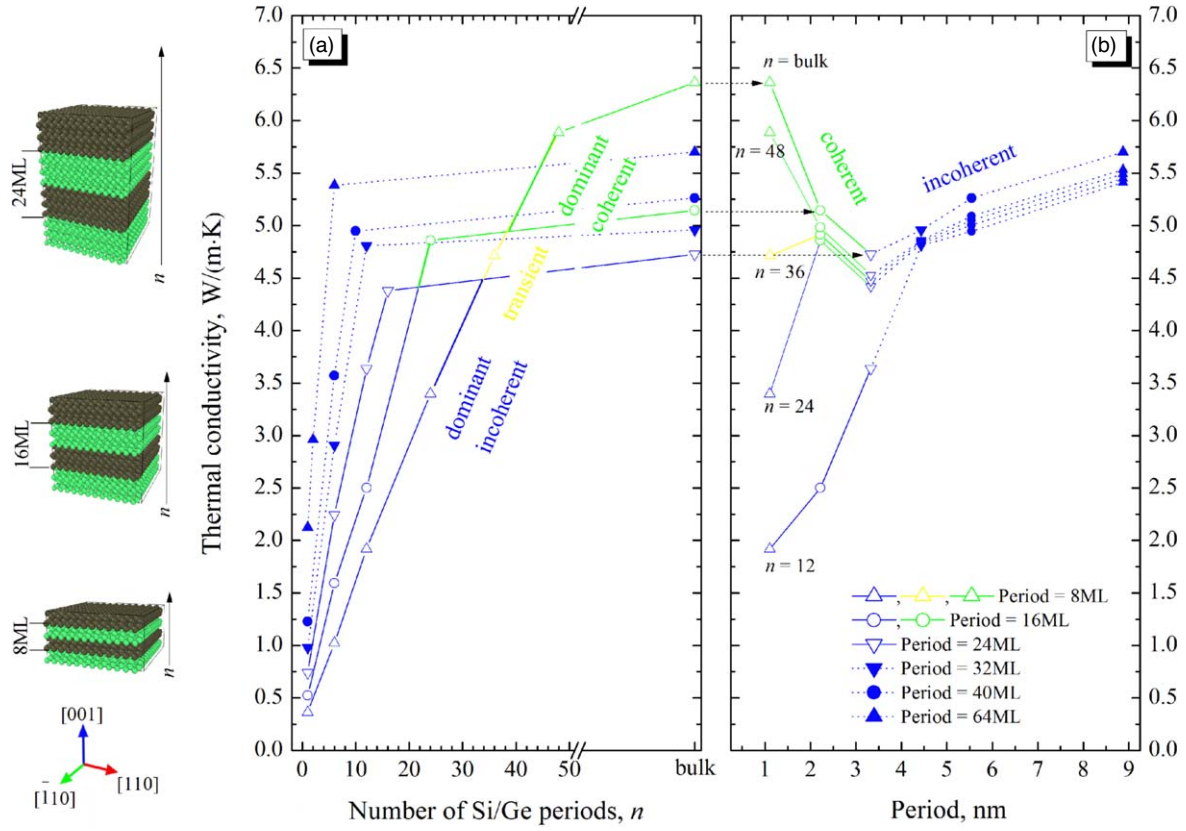

Fig. 8. (Color online) Cross-plane phonon thermal conductivity in the [001] direction at 300 K for the Si/Ge (001) multilayer structures versus the number of periods (a); the period at fixed number of periods (b).

thermal transport is incoherent at any period; at $n = 24$ and 36, it is coherent only at the period of 16 monolayers. At $n = 36$, an additional transition region (yellow) appears due to the fact that the thermal conductivity at the period of 8 monolayers is higher as compared to the 24 monolayer case, but it is still lower than for the 16 monolayer case. For $n > 38$, it can be seen that the graph practically repeats the dependence characteristic of the bulk superlattice.

Our results also state that in multilayer films with a small number of periods incoherent thermal transport dominates, since phonon interference either does not occur, or a certain number of phonons interferes due to a limited amount of interfaces.[50] Moreover, the minimum thermal conductivity is achieved in a superlattice structure when its period and the phonon coherence length are equal.[49] The coherence length, as a characteristic of the spatial expansion of the wave packet, is a size-dependent quantity that decreases with the number of periods in a superlattice structure.[49]

4. Conclusions

The influence of a specific direction on the in- and cross-plane phonon thermal conductivity at 300 K for the (001), (110), and (111) oriented Si/Ge multilayer films was studied by non-equilibrium molecular dynamics in comparison with the homogeneous Si and Ge films of equivalent thickness. The well-resolved orientation effect has been revealed for the in-plane thermal transport as compared to the cross-plane one in the considered Si/Ge multilayer films caused by the predominance of the layer-restricted mode over the extended mode in the thermal conductivity for the in-plane thermal transport and vice versa for the cross-plane one. Thus, the difference in thermal conductivity between the largest and smallest values for the in-plane case can reach as much as about 15 W/(m·K) for one period of the layered film (Fig. 1), and it is only about 1 W/(m·K) for several dozens of periods for the cross-plane case (Fig. 5). Also our results demonstrate a typical decrease in the phonon thermal conductivity with a decrease of the number of periods of the considered structures to occur because of the size effect. In particular, when the number of periods drops from the bulk to one, the thermal conductivity for the (001) orientated films decreases by more than 17 times along the [001] direction for the cross-plane case (Fig. 5) and by almost 4 times along the $[\bar{1}10]$ direction for the in-plane case (Fig. 2).

It is found that investigated Si/Ge multilayer films with respect to their orientation display a crossover in the dependencies of in- and cross-plane thermal conductivities versus the film thickness. For instance, for the cross-plane thermal transport the (001)/[001] direction is characterized by the lowest conductivity among the other structures for the number of periods to be less than 40, while the (111)/[111] direction exhibits the lowest conductivity at a sufficiently large number of periods (more than 40) (Fig. 5). At the same time, for the in-plane transport, such the "switching" from the (001)/$[\bar{1}10]$ direction to the (110)/[001] one occurs at a smaller number of periods ($n = 4$) (Fig. 2). This effect may be ascribed to the difference in the saturation rates of the extended phonon mode in thermal transport, depending on the phonon scattering, in both cross-plane and in-plane directions.

Thus, the data obtained demonstrates that by selecting the period and the number of periods of the Si/Ge multilayer

structures, it is possible to neutralize the negative wave effect, ensuring the dominance of incoherent thermal transport for the cross-plane case (Fig. 8), which is characterized by the lowest thermal conductivity (reaching the amorphous limit). In order to promote such Si/Ge multilayer films for thermoelectric device fabrication, the estimates of their thermoelectric figure of merit, including investigations of the temperature dependence of the phonon thermal conductivity as well as their power factor, should be performed.

Acknowledgments

This work has been supported by the Belarusian National Research Program "Materials Science, New Materials and Technology." D. B. M. acknowledges the support of the MEPhI Program Priority 2030 and the resources of NRNU MEPhI high-performance computing center.

1) Y. Li, G. Wang, M. Akbari-Saatlu, M. Procek, and H. H. Radamson, Front. Mater. **8**, 611078 (2021).
2) H. R. Shanks, P. D. Maycock, P. H. Sidles, and G. C. Danielson, Phys. Rev. **130**, 1743 (1963).
3) A. F. Ioffe, Can. J. Phys. **34**, 1342 (1956).
4) J. A. Pérez-Taborda, O. Caballero-Calero, and M. Martín-González, *New Research on Silicon—Structure, Properties, Technology* (InTechOpen, London, 2017) p. 183.
5) C. J. Gomes, M. Madrid, J. V. Goicochea, and C. H. Amon, J. Heat Transfer **128**, 1114 (2006).
6) X. Wang and B. Huang, Sci. Rep. **4**, 6399 (2014).
7) M. Maldovan, J. A. Phys. **125**, 224301 (2019).
8) P. Heino, E. Phys. J. B **60**, 171 (2007).
9) Z. Aksamija and I. Knezevic, Phys. Rev. B **82**, 045319 (2010).
10) H. Karamitaheri, N. Neophytou, and H. Kosina, J. Appl. Phys. **113**, 204305 (2013).
11) X. Zhang and X. Wu, Comput. Mater. Sci. **123**, 40 (2016).
12) Z. H. Wang and M. J. Ni, Heat Mass Transfer **47**, 449 (2011).
13) A. L. Khamets, I. I. Khaliava, I. V. Safronov, A. B. Filonov, and D. B. Migas, Phys. Solid State **5**, 541 (2022).
14) E. S. Landry and A. J. H. McGaughey, Phys. Rev. B **79**, 075316 (2009).
15) J. Garg and G. Chen, Phys. Rev. B **87**, 140302 (2013).
16) K.-H. Lin and A. Strachan, Phys. Rev. B **87**, 115302 (2013).
17) Z. Aksamija and I. Knezevic, Phys. Rev. B **88**, 155318 (2013).
18) K. Kothari and M. Maldovan, Sci. Rep. **7**, 5625 (2017).
19) H. Dong, B. Wen, Y. Zhang, and R. Melnik, RSC Adv. **7**, 29959 (2017).
20) A. Kandemir, A. Ozden, T. Cagin, and C. Sevik, Sci. Technol. Adv. Mater. **18**, 187 (2017).
21) G. P. Srivastava and L. O. Thomas, Nanomaterials **10**, 673 (2020).
22) S.-M. Lee, D. G. Cahill, and R. Venkatasubramanian, Appl. Phys. Lett. **70**, 2957 (1997).
23) T. Borca-Tasciuc et al., Superlat. Microstruct. **28**, 199 (2000).
24) W. L. Liu, T. Borca-Tasciuc, G. Chen, J. L. Liu, and K. L. Wang, J. Nanosci. Nanotech. **1**, 39 (2001).
25) S. Chakraborty, C. A. Kleint, A. Heinrich, C. M. Schneider, J. Schumann, M. Falke, and S. Teichert, Appl. Phys. Lett. **83**, 4184 (2003).
26) J. A. Perez Taborda, J. J. Romero, B. Abad, M. Muñoz-Rojo, A. Mello, F. Briones, and M. S. Martin Gonzalez, Nanotechnology **27**, 175401 (2016).
27) V. Samvedi and V. Tomar, J. Appl. Phys. **105**, 013541 (2009).
28) A. Malhotra, K. Kothari, and M. Maldovan, J. Appl. Phys. **125**, 044304 (2019).
29) Jmol: an open-source Java viecer for chemical structures in 3D: (http://jmol.org/) https://jmol.sourceforge.net/#:~:text=Jmol%20is%20a%20free%2C%20open,%2C%20and%20Linux%2FUnix%20systems.
30) A. Stukowski, Modelling Simul. Mater. Sci. Eng. **18**, 015012 (2009).
31) S. Plimpton, J. Comp. Phys. **117**, 1 (1995).
32) J. Tersoff, Phys. Rev. B **39**, 5566 (1989).
33) Y. He, I. Savić, D. Donadio, and G. Galli, Phys. Chem. Chem. Phys. **14**, 16209 (2012).
34) Z. Wang, Mater. Today Commun. **22**, 100822 (2020).
35) A. Giri, J. L. Braun, and P. E. Hopkins, J. Appl. Phys. **119**, 235305 (2016).
36) A. Carreras, (2021), phonoLAMMPS: A python interface for LAMMPS phonon calculations using phonopy (0.8.1), *Zenodo* (https://doi.org/10.5281/zenodo.5668319). https://zenodo.org/record/5668319#.Y7m4TVxBztQ.
37) A. Togo and I. Tanaka, Scr. Mater. **108**, 1 (2015).
38) H. Zhu, C. Zhao, P. Nan, X.-M. Jiang, J. Zhao, B. Ge, C. Hiao, and Y. Xie, Chem. Mater. **33**, 1140 (2021).
39) H. Xie, Materials Lab **1**, 220051 (2022).
40) F. X. Alvarez, J. Alvarez-Quintana, D. Jou, and J. Rodriguez Viejo, J. Appl. Phys. **107**, 084303 (2010).
41) D. P. Sellan, J. E. Turney, A. J. H. McGaughey, and C. H. Amon, J. Appl. Phys. **108**, 113524 (2010).
42) K. E. Goodson, Science **315**, 342 (2007).
43) E. S. Landry and A. J. H. McGaughey, J. Appl. Phys. **107**, 013521 (2010).
44) K. Kothari, A. Malhotra, and M. Maldovan, J. Phys.: Condens. Matter **31**, 345301 (2019).
45) X. Mu, L. Wang, X. Yang, P. Zhang, A. C. To, and T. Luo, Sci. Rep. **5**, 16697 (2015).
46) X. Mu, T. Zhang, D. B. Go, and T. Luo, Carbon **83**, 208 (2015).
47) S. Tamura, Y. Tanaka, and H. J. Maris, Phys. Rev. B **60**, 2627 (1999).
48) M. V. Simkin and G. D. Mahan, Phys. Rev. Lett. **84**, 927 (2000).
49) B. Latour, S. Volz, and Y. Chalopin, Phys. Rev. B **90**, 014307 (2014).
50) P. Chakraborty, L. Cao, and Y. Wang, Sci. Rep. **7**, 8134 (2017).
51) Y. Chen, D. Li, J. R. Lukes, Z. Ni, and M. Chen, Phys. Rev. B **72**, 174302 (2005).